Anais XI SBSR, Belo Horizonte, Brasil, 05 - 10 abril 2003, INPE, p. 2241 - 2248.

EXTRACTION OF SPATIAL PATTERNS IN TROPICAL RAINFOREST FROM POWER SPECTRUM ANALYSIS OF AIRBORNE SAR DATA

TILL NEEFF [1,2]
LUCIANO VIEIRA DUTRA [1]
JOÃO ROBERTO DOS SANTOS [1]
CORINA DA COSTA FREITAS [1]
LUCIANA SPINELLI ARAUJO[1]

[1]INPE – Instituto Nacional de Pesquisas Espaciais
Caixa Postal 515 - 12201-970 - São José dos Campos - SP, Brasil
{tneeff, dutra, corina}@dpi.inpe.br, {jroberto, lucian}@ltid.inpe.br

[2]UCB – University of California at Berkeley
94720 Berkeley, CA, USA
tneeff@nature.berkeley.edu

Abstract. Power spectrum analysis is used for analysis of spatial forest structure from airborne X-band SAR data in the Brazilian Amazon. Spectral estimates are arrived at empirically by periodograms, from autoregressive moving-average models, and from a window-based autocorrelation function. The spectral estimates derived from SAR data are validated with those derived from ground data with exact locational match. The results gotten by ARMA modeling, and by the correlogram method do reveal particularly good correspondence between remote sensing and reference data, repeating patterns at the pixel level can be detected in the images. These patterns seem to arise from canopy structure, and thus allow for extraction of parameters of spatial forest structure, particularly of forest density.

Keywords: radar, power spectrum analysis, spectral estimation, forest structure, autocorrelation

1 Introduction

The analysis of image texture is stipulated to provide an indispensable contribution to forest characterization from remote sensing data (St-Onge and Cavayas 1995), and thus to its ecological assessment for ecosystem management (Song and Woodcock 2002). Use of second order statistics has especially been recommended for mapping of canopy structure, of crown size and forest density (Song and Woodcock 2002). A number of research efforts has shown the shape features of variograms (i.e. range, sill, nugget) to be related to the forest parameters of interest, the variance structure beyond the range of the variograms has not yet been accounted for, e.g. St-Onge and Cavayas (1995), St-Onge and Cavayas (1997), Muinonen et al. (2001) Song and Woodcock (2002).

A lot of work has been done on exploring spatial structure of forests by approaches that are local in the sense that they apply to small sub-areas of the image, for instance by moving windows and local statistics, i.e. Wulder et al. (2000), Sheng et al. (2001), Tarp-Johansen (2002). A different approach that builds on essentially taking the image as spectral object, rather than spatial object is getting more attention, e.g. Sommerfeld et al. (2000).

In this paper an exact locational match of remote sensing and radar data is used to conduct power spectrum analysis on airborne X-band SAR data. While other forest parameters (biomass, mean diameter, basal area, etc.) have been mapped from these same data with good precision, forest density is quite difficult to measure (Santos et al. 2002a), (Neeff et al. 2002a), (Neeff et al. 2002b). The spectral estimates are related to the crown-structure of primary forest.

Profiles of pixel values from the image display sinusoidal shapes. Similarly, an autocorrelation function as gotten from a moving window in the image is observed to have a sinusoidal shape, indicating repeating patterns coinciding with crown texture in the image. Spectral estimates derived from both pixel profiles and the window-based autocorrelation function are related to those derived from ground data, namely forest transects. For ground data ARMA modeling and empirical methods are used, the image data furthermore is investigated by the correlogram method.

2 Material and methods

2.1 Study area

The study area is situated in the Tapajós Nationalpark south of Santarém in the Brazilian Amazon, between W 58°50'41.68'' through 59°07'57.18'', and S 3°15'19.4'' through 3°15'16.99''. The climate according to Köppen is Amw with an average monthly rainfall of 1,750 to 2,000 mm and a yearly temperature average of 26 °C.

2.2 Data collection

Extensive field work has been conducted to collect data on primary forests in 2000 as described in Santos et al. (2002b). A total of 9 plots is measured, in transects of 250 x 10 m. Tree positions, species, diameters at breast height $d_{1.3}$ above 10 cm, and corresponding total tree heights are measured.

An area of approximately 1,300 km^2 was mapped in the end of 2000. The data have been collected by the airborne AeS-1 sensor (Aerosensing Radarsysteme GmbH, Germany), which makes use of synthetic aperture radar (SAR) technology (Schwäbisch and Moreira 1999). It operates on X-band with HH polarization and fully polarimetric on P-band. In this study only the X-band data is used: polarization HH; 9.6 GHz operating frequency; 400 MHz bandwidth; 1.8 m baseline; 0.5 m horizontal resolution; depression angle 45°; mean height 3,216 m.

2.3 Spectral estimation

Data which is organized in a serial way can be analyzed based on the assumption that it is made up of sine and cosine waves with different frequencies and amplitudes. This approach is common for the analysis of time series and in signal processing. The estimation of the spectrum of such series provides information on periodicities in the data (Box and Jenkins 1970), (Marple Jr. 1987). In this study three devices are used for spectral estimation: the periodogram, the correlogram, and the theoretical spectral density function of fitted ARMA models.

The periodogram is a function of the frequency, and derives power from the amplitudes of a fitted Fourier series model. It is computed from the original data values (Box and Jenkins 1970):

$$z_t = \alpha_0 + \sum_{i=1}^{(N-1)/2} \left(\alpha_i \cos 2\pi f_i t + \beta_i \sin 2\pi f_i t \right) + \varepsilon_t$$

$$I(f_i) = \frac{N}{2}\left(\hat{\alpha}_i + \hat{\beta}_i \right), \qquad i = 1, 2, \ldots, (N-1)/2$$

The correlogram is the Fourier cosine transform of the autocorrelation function with estimated autocorrelation ρ_k at lag k (Box and Jenkins 1970), (Marple Jr. 1987). In order to avoid the high variance of higher lags, only a number of lags limited to the first 20% is used, and the higher lags are set to zero. The data values themselves are not directly used for derivation:

$$I(f_i) = 2\left\{ 1 + 2\sum_{K=1}^{N-1} r_k \cos 2\pi f_i k \right\}$$

The theoretical spectral density function of a fitted ARMA(p,q) model is given with σ^2 as the variance of the white noise process, φ and θ as the parameter vectors of the model, and with $j = \sqrt{-1}$ (Marple Jr. 1987). The spectral density thus only is a function of the fitted model coefficients:

$$I(f_i) = s^2 \left| \frac{1 + \sum_{l=1}^{p} q_l \exp(-j2pf_i l)}{\sum_{l=1}^{q} j \exp(-j2pf_i l)} \right|^2$$

Box and Jenkins (1970) give general criteria for model selection in autoregressive moving-average modelling according to the shape of autocorrelation function and partial autocorrelation function. Model fitting here draws on these general rules, and initially fits a high order mixed model ARMA(16,16) to all data points. All parameters are tested for significance, and after dropping the non-significant parameters, model fit is optimized.

2.4 Recoding of ground data

In the original ground data, trees are located in planar coordinates, with the x-coordinate ranging between 0-250 m, and the y-coordinate between 0-10 m. In order to apply the techniques of one-dimensional spectral estimation, the ground data are transformed to the format of a signal. Given its small extension, possibly below the size of individual trees, the y-coordinate is omitted. The new signal is constructed to be sampled at an interval of one meter, and its amplitude is gotten from the diameter of the strongest tree at the corresponding position. For the case of missing values, i.e. at positions, where no trees have been measured in the ground data, a filter is sequentially applied, until all zeros are eliminated.

$$z'(i) = \max\{z(j)\}; \qquad i = 0,1,2,...,I; \qquad 0 \le j \le J;$$

$$z'(i) = \max\{z(i-1), z(i+1)\}; \qquad \forall\{z(i) \mid z(i) = 0\}.$$

2.5 Computation of autocorrelation for image data

An unbiased estimator of the kth lag autocorrelation ρ_k is given by (Marple Jr. 1987):

$$r_k = \frac{c_k}{c_0}, \qquad \textit{where}$$

$$c_k = \frac{1}{N-k} \sum_{t=1}^{N-k} (z_t - \bar{z})(z_{t+k} - \bar{z}), \qquad k = 0,1,2,..., K.$$

In this formulation application to image data would be limited to just taking a single line of pixels to extract autocorrelation from an image. Therefore the result is modified for the case of computing the autocorrelation based on a pixel window which is moved over an image, where the window used is of dimensions (IxJ) = (5x5).

3 Results

3.1 Analysis of ground data

In figure 1 the main steps of the recoding of ground data to signal format are sketched. The autocorrelation function of the new data set appears to be dominated by damped sinusoidal waves, there is no indication for a finite structure, but the function seems to be infinite. A local-regression smoother applied to the ground data reveals some periodic structure (see figure 2a). The spectral estimates for these are derived, namely the periodogram and the theoretical spectral density function of autoregressive moving average models (see figure 2b).

3.2 Analysis of radar data

At locations in the image exactly corresponding to those of the field transects, a profile line of pixel values is extracted. In figure 3a an example profile is drawn together with a local-regression smoother. There is some sinusoidally repeating pattern with a cycle of about 30-40 m recognizable. Both periodogram and ARMA models of the pixel strip are used to extract the frequency of the patterns in the profile values (figure 3b).
In figure 4 spectral estimation for radar image data by use of the correlogram is displayed. The autocorrelation functions as computed from pixel windows moved sequentially over the image at locations corresponding to the ground data transects reveal a typical sinusoidal shape of regularly alternating maxima and minima. To visually enhance this pattern, local regression smoothers are used. The distances between maxima amounts to roughly 20 m. The autocorrelation function yields the correlogram as spectral estimate. The typical shape of the correlograms is exemplified by figure 4b.

3.3 Relation of ground data and forest structure

Figure 5 interprets the significance of spectral estimates for ground data that are transformed to signal format. Even though some relation to forest density would be expected, the scatterplot of the number of individuals per hectare versus the distance corresponding to the prime maxima of the spectra does not reveal any obvious relationship (figure 5a).
However, the distances of the spectra's prime maxima correspond to the average distances between a sub-collective of the strongest individuals, this is illustrated in figure 5b. The sub-collective consists in roughly the strongest 25% of all individuals. This fraction is quite constant for all samples. None would deviate by more than one standard deviation.

3.4 Relation of remote sensing data and ground data

The two different methods for spectral estimation of the ground data and the three different methods for spectral estimation of the radar data are compared. For the ground data the periodogram and the theoretical spectral density function of fitted ARMA models are taken into account, and for the radar data the periodogram, the theoretical spectral density function of the fitted ARMA models, and the correlogram, are used. A visual comparison reveals similar behaviour over the whole spectra in all frequency ranges (figure 6). Maxima of spectral density in the data from the different sources are visually identified, and the corresponding maxima are matched. of particularly interest is the position of the low-frequency prime maxima.
The distances that correspond to prime maxima of the spectra are extracted from the spectral density functions. Between two sets of spectral estimates for ground data and three sets of estimates from radar data six linear regression models are build. The three best of them are graphically displayed in figure 7.
All six models are summarized in table 1. The models that both yield high determination coefficients r^2 , and who do not differ significantly from the diagonal line are considered 'good' models. The ground data can be modeled by both the empirical periodogram, and by ARMA models. However, the ARMA models might be preferred. Best estimates of spectral density from radar data are gotten by the correlograms of the window-based autocorrelation function. The best model relates an ARMA model from ground data to the correlogram from remote sensing data, its determination coefficient attains a value of $r^2 = 0.61$.

Table 1: Regression parameters for prime maxima of spectra from ground data and remote sensing data. Displayed are periodogram, ARMA and correlogram methods for derivation of spectra from remote sensing data, and periodogram and ARMA method for ground data.

GD/SAR	*periodogram*	*ARMA*	*correlogram*
periodogram	0.17	0.3	0.43
ARMA	0.6	0.05	0.61

4 Discussion

Power spectrum analysis is successfully used as a tool for the remote sensing of forest parameters from radar data. The adopted approach substitutes time for space and uses standard tools of time series modelling and digital signal processing to analyse forest structure. This approach is novel for forest analysis from remote sensing data and may provide basis for much more extended use, than demonstrated here. The spectra as obtained from radar data match those obtained from ground data, establishing the basis for further use of this relationship.

Good concordance has been gotten from the spectral estimates derived from the window based autocorrelation function by the correlogram method. The analysis of just pixel strips has not yielded convincing results. Main interest lies here on the position of the low-frequency 'prime' maxima, these maxima are taken to correspond to the average distances between the individuals of the dominating tree collective.

Crowns can be expected to display somewhat similarly in remote sensing data, which among other applications is the basic assumption in methods of template matching (e.g. Tarp-Johansen (2002)). Cohen and Spies (1990) therefore observe that profiles of pixel values have sinusoidal shape with alternating maxima and minima, whose distances correspond to some repeating pattern. The same observations are made here, and the patterns are even clearer for pixel windows which are correlated at distances that correspond to average tree distances. Thus the window-based autocorrelation functions are observed to have a sinusoidal shape with alternating maxima and minima. Power spectrum analysis is the appropriate tool for extracting these distances, and the results contain important ecological information.

Neeff et al. (2002a) showed that only a dominating collective of all tree individuals is visible in X-band SAR data. Obviously the distances obtained here mainly > 15 m do also belong to some strongest subset of all tree individuals. Similar results have been obtained by Dutra et. al. (2002). The hypothesis that prime maxima from spectra correspond to distances between trees of a dominant collective is verified by a simple approach that calculates average distances between tree individuals above some threshold size. The dominating collective bearing on the prime maxima of the spectral estimates from X-band SAR images in this case is estimated to correspond to a quarter of all individuals.

Performing spatial analysis on forests, this dominant collective is of major interest. Successional cycles and forest turnover rates are driven by the life cycles of the biggest trees Finegan (1996), and their tree fall gaps determine the composition and structure of forest communities (Brokaw 1982), (Wirth et al. 2001). The spatial structure of forest regarding the major individuals is receiving more attention (Keller et al. 2001). Analysis of such forest structure by texture information from from remote sensing data is attributed interest for global change studies (Weishampel et al. 2001). The approach adopted here may provide a means for investigation of issues like the structure of forest with spatio-temporal dimension.

5 Acknowledgements

The authors acknowledge CNPq (grants 301400/91-1(PV), 300677/91-0, 380597/99-3, 300927/92-4), FAPEMIG (grant CRA 00054/00) support, and funds from the MCT (Brazilian Ministery of Science and Technology), within its Program ‘Science & Technology for Environmental Studies’. The authors wish to thank the 8th BEC (Brazilian Army), IBAMA/MMA and SUDAM for logistic support. This research is a partial result of LBA LC-11 project, and also of the scientific cooperation between INPE (National Institute for Space Research), DSG (Brazilian Army Geographical Service), and UCB (University of California at Berkeley).

6 References

Box, G. and G. Jenkins (1970). Time Series Analysis: Forecasting and Control. Oakland, USA: Holden-Day Incorporated. p. 575.

Brokaw, N. (1982). The definition of treefall gap and its effect on measures of forest dynamics. Biotropica 14 (2), 158-160.

Cohen, W. and T. Spies (1990). Semivariograms of digital imagery for analysis of conifer canopy structure. Remote Sensing of Environment 34, 167-178.

Dutra, L., M. Elmiro, C. Freitas, J. Santos, J. Mura, L. Araujo, P. Albuquerque, and T. Neeff (2002). Estimation of digital height model (DHM) of tropical forest by using dual frequency InSAR methodology. International Journal of Remote Sensing. Submitted.

Finegan, B. (1996, March). Pattern and process in neotropical secondary rain forests: the first 100 years of succession. Trends in Ecology & Evolution 11 (3), 119-124.

Keller, M., M. Palace, and G. Hurtt (2001). Biomass estimation in the Tapajós national forest, Brazil examination of sampling and allometric uncertainties. Forest Ecology and Management 154, 37-{382.

Marple Jr., S. (1987). Digital Spectral Analysis with Applications. Englewood Cliffs, USA: Prentice-Hall Incorporated. p. 492.

Muinonen, E., M. Maltamo, H. Hyppänen, and V. Vainikainen (2001). Forest stand characteristics estimation using a most similar neighbor approach and image spatial structure information. Remote Sensing of Environment 78, 223-228.

Neeff, T., L. Dutra, J. dos Santos, C. Freitas, and L. Araujo (2002b). Tropical forest stand table modelling from airborne SAR data. submitted to Forest Ecology and Management.

Neeff, T., L. Dutra, J. Santos, C. Freitas, and L. Araujo (2002a). Tropical forest biomass measurement by backscatter and DEM information as derived from airborne SAR. submitted to Forest Science.

Santos, J., L. Araujo, C. Freitas, L. Soler, F. Gama, and L. Dutra (2002a, September 23-27). Analysis of forest biomass variation in the Amazon and its' influence on the response of P-band SAR polarimetric data. In Proceedings 9th International Symposium on Remote Sensing, Crete, Greece.

Santos, J., M. Lacruz, L. Araujo, and M. Keil (2002b). Savanna and tropical rainforest biomass estimation and spatialization using JERS-1 data. International Journal of Remote Sensing 23 (7), 1217-1229.

Schwäbisch, M. and J. Moreira (1999, 21-24th June). The high resolution airborne interferometric SAR AeS-1. In Proceedings, 21th Canadian Symposium on Remote Sensing, Ottawa, Canada. p. 8.

Sheng, Y., P. Gong, and G. Biging (2001). Model-based conifer-crown surface reconstruction from high-resolution aerial images. Photogrammetric Engineering and Remote Sensing 67 (8), 957-965.

Sommerfeld, R., J. Lundquist, and J. Smith (2000). Characterizing the canopy gap structure of a disturbed forest using the fourier transform. Forest Ecology and Management 128, 101-108.

Song, C. and C. Woodcock (2002). The spatial manifestation of forest succesion in optical imagery: the potential of multiresolution imagery. Remote Sensing of Environment 82, 271-284.

St-Onge, B. and F. Cavayas (1995). Estimating forest stand strucutre from high resolution imagery using the directional variogram. International Journal of Remote Sensing 16, 1999-2021.

St-Onge, B. and F. Cavayas (1997). Automated forest structure mapping from high resolution imagery based on directional semivariogram estimates. Remote Sensing of Environment 61, 82-95.

Tarp-Johansen, M. (2002). Automatic stem mapping in three dimensions by template matching from aerial photographs. Scandinavian Journal of Forest Research 17 (4), 359-368.

Weishampel, J., J. Godin, and G. Henebry (2001). Pantropical dynamics of 'intact' rain forest canopy texture. Global Ecology & Biogeography 10, 389-397.

Wirth, R., B. Weber, and R. Ryel (2001). Spatial and temporal variability of canopy structure in a tropical moist forest. Acta Oecologica 22, 235-244.

Wulder, M., K. Niemann, and D. Goodenough (2000). Local maximum filtering for the extraction of tree locations and basal area from high spatial resolution imagery. Remote Sensing of the Environment 73, 103-114.

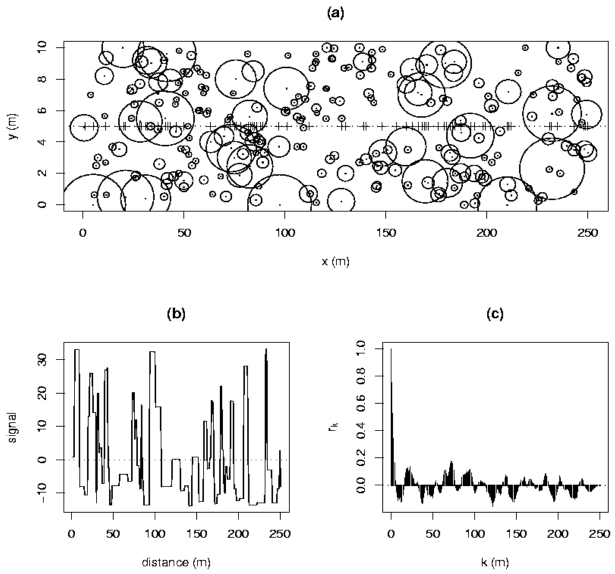

Figure 1: Transformation of field data to signal format. (a) schematic representation of example plot (sample # 1), with horizontal positions of trees $d_{1.3} > 10$ cm marked. Size of circles corresponds to $d_{1.3}$ of trees. (b) recoded signal and filtered with mean subtracted. (c) autocorrelation function of signal.

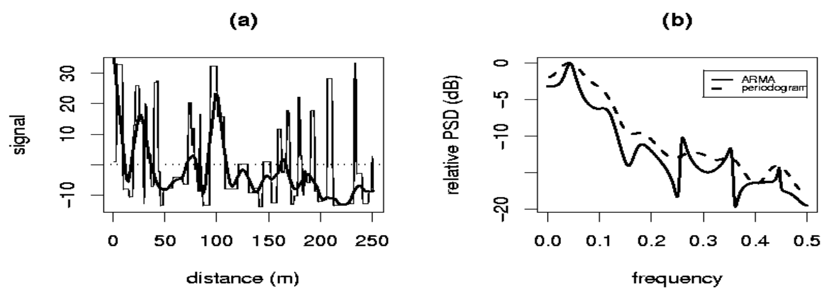

Figure 2: Spectral estimation from ground data. (a) transformed forest ground data in signal format with local-regression smoother. (b) estimates for example forest transect as derived by two different estimators: periodogram, and theoretical power spectral density of fitted ARMA model. Maximum frequency corresponds to two units of measurement, i.e. 2 m.

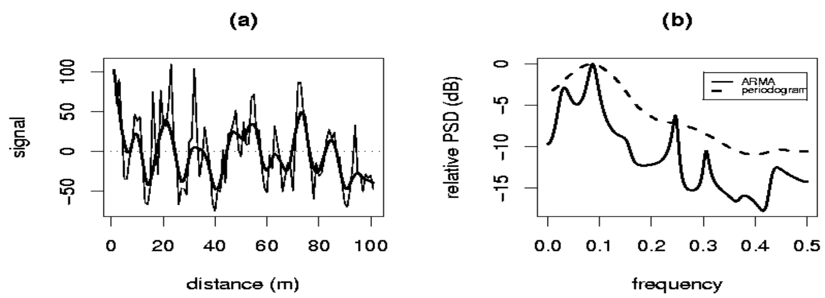

Figure 3: Power Spectrum Analysis of a profile of pixel values from X-band radar imagery. (a) profile of radar amplitudes with mean removed, and with local regression smoother; (b) spectral estimates for profile, periodogram and ARMA model. Maximum frequency corresponds to two pixels, i.e. 5 m per cycle.

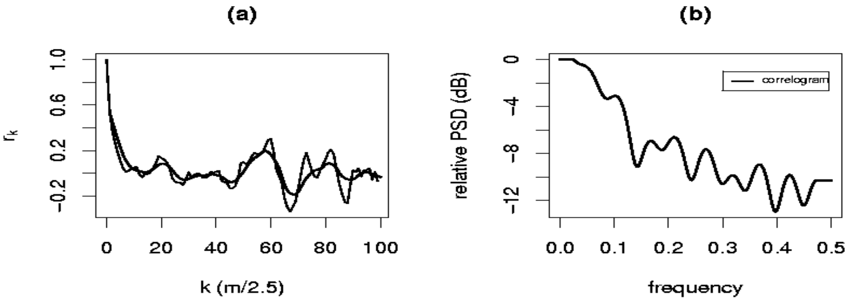

Figure 4: Use of Correlogram for spectral estimation from radar image. (a) Autocorrelation function from moving-window with local-regression smoother. Lags k correspond to pixel size 2.5 m, r_k is kth lag estimated autocorrelation. (b) Spectral estimate by correlogram: Maximum frequency corresponds to two pixels, i.e. 5 m per cycle.

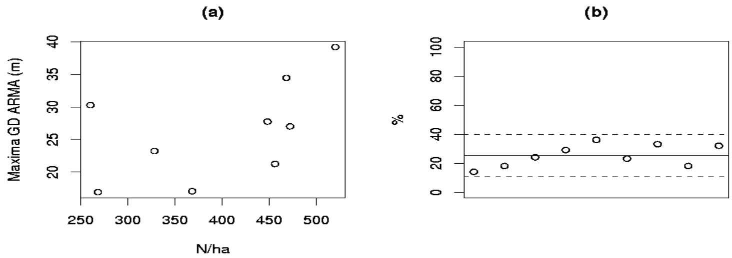

Figure 5: Relation of results of spectral modeling of ground data to forest density. (a) scatterplot of number of individuals per hectare and prime maxima from spectral estimation by ARMA of ground data. (b) percentage of strongest tree individuals whose average distance corresponds to prime maxima from ARMA modeling of ground data, samples in arbitrary order (straight line - mean, dotted lines - standard deviation).

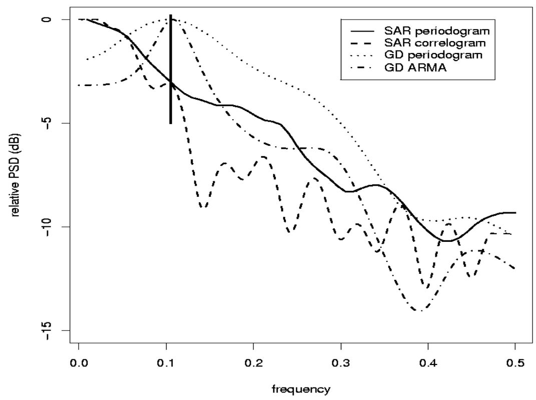

Figure 6: Relation between spectral estimates of ground data and of remote sensing data. Displayed are for the ground data the periodogram, and the theoretical spectral density function of the fitted ARMA model. For the radar data both the periodogram, and the correlogram are displayed. The prime maximum is marked with a vertical line at frequency 0.105. Frequency scale of ground data is assimilated to scale of remote sensing data, frequencies below 0.2 cycles per pixel, i.e. below 5 m are omitted.

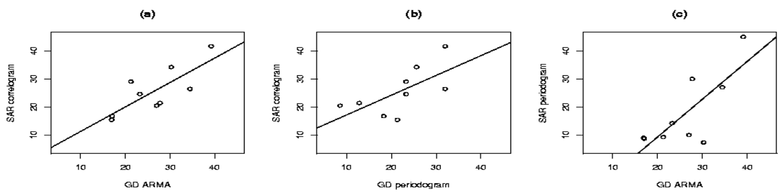

Figure 7: Scatterplot with regression models for prime maxima of spectral estimates from ground data and radar data by various methods. Radar data (SAR) as dependent variable, and ground data (GD) as independent variable. All units in meters.